Three-body Casimir effects and nonmonotonic forces

Three-body Casimir effects and nonmonotonic forces

Pablo Rodriguez-Lopez,[1] Sahand Jamal Rahi,[2] and Thorsten Emig[3,4]
[1]*Departamento de Fisica Aplicada I and GISC, Universidad Complutense, 28040 Madrid, Spain*
[2]*Massachusetts Institute of Technology, Department of Physics, 77 Massachusetts Avenue, Cambridge, Massachusetts 02139, USA*
[3]*Institut für Theoretische Physik, Universität zu Köln, Zülpicher Strasse 77, 50937 Köln, Germany*
[4]*Laboratoire de Physique Théorique et Modèles Statistiques, CNRS UMR 8626, Université Paris-Sud, 91405 Orsay, France*
(Received 4 May 2009; published 31 August 2009)

Casimir interactions are not pairwise additive. This property leads to collective effects that we study for a pair of objects near a conducting wall. We employ a scattering approach to compute the interaction in terms of fluctuating multipoles. The wall can lead to a nonmonotonic force between the objects. For two atoms with anisotropic electric and magnetic dipole polarizabilities, we demonstrate that this nonmonotonic effect results from a competition between two- and three-body interactions. By including higher-order multipoles we obtain the force between two macroscopic metallic spheres for a wide range of sphere separations and distances to the wall.

DOI: 10.1103/PhysRevA.80.022519 PACS number(s): 31.30.jh, 03.70.+k, 42.25.Fx, 42.50.Lc

A hallmark property of dispersion forces is their nonadditivity which clearly distinguishes them from electromagnetic forces between charged particles [1]. Investigations of the interactions between multiple objects are limited mostly to atoms or small particles which are described well in dipole approximation [2]. This approximation cannot be used for macroscopic objects at separations that are comparable to their size since higher-order multipole fluctuations have to be included [3,4]. In such situations, also other common "additive" methods such as proximity or two-body-interaction approximations fail. Recently, three-body interactions between macroscopic bodies, including those resulting from higher multipoles, have been studied in geometries that are composed of two parallel perfect metal cylinders of quadratic [5] or circular [6,7] cross section and one or two parallel sidewalls. In these quasi-two-dimensional (2D) geometries the forces between pairs of objects have been found to vary nonmonotonically with the separation from the other object(s). The nonmonotonicity of the forces results from a competition between transverse magnetic (TM) and transverse electric (TE) modes. In this paper we study nonmonotonic effects beyond the dipole approximation by including higher-order mulitpole fluctuations. This allows us to compute three-body interactions between *macroscopic* objects, extending previous work that is limited to atoms and molecules [2]. We investigate collective three-body effects between *compact* objects, including anisotropic polarizabilities, and a wall in three dimensions using a recently developed scattering approach [4,8]. There are precursors of and contributions to the scattering approach, see, e.g., [9–12]. This approach allows us to observe the influence of polarization coupling and anisotropy on nonmonotonic effects. We find that the force between atoms and macroscopic spheres depends, again, nonmonotonically on the separation of the sidewall, and we provide a simple physical argument using image fluctuations to explain this.

We consider the retarded Casimir interaction between a pair of polarizable objects with anisotropic electric and magnetic polarizabilities near a conducting wall, see Fig. 1. We identify a competition between two- and three-body effects and prove that this leads to a nonmonotonic dependence of the force between the objects on the wall separation H for *each* of the four possible polarizations of fluctuations (electric or magnetic and parallel or perpendicular to the wall) *separately*. For isotropic polarizabilities we find that only the force component due to electric fluctuations is nonmonotonic in H.

For atoms, magnetic effects are almost always rather small in the retarded limit. Contrary to this, for conducting macroscopic objects contributions from electric and magnetic multipole fluctuations are comparable. To study the effect of higher-order multipoles, we consider also two perfect metal spheres near a wall, see Fig. 1. Based on consistent analytical results for large separations and numerical computations at smaller distances we find a nonmonotonic dependence of the force between the spheres on H. Unlike for atoms, this effect occurs at sufficiently large sphere separations only.

As presented in Ref. [8] the Casimir energy of two bodies in the presence of a perfectly conducting sidewall can be obtained using the scattering approach by employing the method of images, which introduces fluctuating currents on the mirror bodies. The Casimir energy of the original system is then given by the energy of the original and the image

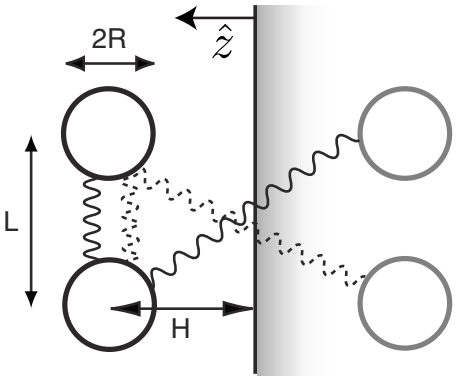

FIG. 1. Geometry of the two-sphere or atom and sidewall system. Shown are also the mirror images (gray) and two- and three-body contributions (solid and dashed curly lines, respectively).

objects, and it can be expressed as an integral over imaginary wave number,

$$\mathcal{E} = \frac{\hbar c}{2\pi}\int_0^\infty d\kappa \ln\det(\mathbb{M}\mathbb{M}_\infty^{-1}), \tag{1}$$

with the matrix

$$\mathbb{M} = \begin{pmatrix} \mathbb{T}^{-1} + \mathbb{U}^{I,11} & \mathbb{U}^{12} + \mathbb{U}^{I,12} \\ \mathbb{U}^{21} + \mathbb{U}^{I,21} & \mathbb{T}^{-1} + \mathbb{U}^{I,22} \end{pmatrix}, \tag{2}$$

which is given by the $\mathbb{T}$ matrix that relates the regular and scattered electromagnetic (EM) fields for each body and by the $\mathbb{U}$ matrices that describe the interaction between the multipoles of object α and object β, $\mathbb{U}^{\alpha\beta}$, and between the multipoles of object α and the image of object β, $\mathbb{U}^{I,\alpha\beta}$. The $\mathbb{T}$ matrices depend only on the properties of the individual bodies such as polarizability, size, and shape. The $\mathbb{U}$ matrices depend only on the distance vector between the objects and decay exponentially with distance and wave number κ. The matrix M_∞ accounts for the subtraction of the object's self-energies and hence follows from $\mathbb{M}$ by taking the limit of infinite separations, i.e., by setting all $\mathbb{U}$ matrices to zero. For a multipole expansion the matrix elements are computed in a vector spherical basis for the EM field with partial wave numbers $l \geq 1$, $m=-l,\ldots,l$. (Details of this expansion and the $\mathbb{U}$-matrix elements can be found in Ref. [8].)

In the following we study the force $F=-\partial\mathcal{E}/\partial L$ between the two objects at separation L and hence eliminate the contributions to the energy that depend only on the sidewall separation H, see Fig. 1. We expand the determinant of Eq. (1) as

$$\begin{aligned}\det(\mathbb{M}\mathbb{M}_\infty^{-1}) = {}& \det(1+\mathbb{T}\mathbb{U}^I)\det(1+\mathbb{T}\mathbb{U}^I) \\ & \times\det[1-(1+\mathbb{T}\mathbb{U}^I)^{-1}\mathbb{T}(\mathbb{U}^{21}+\mathbb{U}^{I,21}) \\ & \times(1+\mathbb{T}\mathbb{U}^I)^{-1}\mathbb{T}(\mathbb{U}^{12}+\mathbb{U}^{I,12})].\end{aligned} \tag{3}$$

The first two determinants on the rhs yield together twice the interaction energy between a single object and the sidewall since $\mathbb{U}^I \equiv \mathbb{U}^{I,11} = \mathbb{U}^{I,22}$ describes the multipole coupling between one object and its image and hence depends only on H. Hence, we consider only the energy $\mathcal{E}_{\circ\circ}$ that corresponds to the last determinant of Eq. (3) and provides the potential energy of the two objects in the presence of the sidewall so that $F=-\partial\mathcal{E}_{\circ\circ}/\partial L$. In the absence of the sidewall, $H\to\infty$, the matrices $U^{I,\alpha\beta}$ all vanish and $\mathcal{E}_{\circ\circ}$ simplifies to the energy between two spheres [4]. For an interpretation in terms of multiple scatterings, it is instructive to use the relation ln det=Tr ln and to Taylor expand the logarithm and the inverse matrices,

$$\begin{aligned}\mathcal{E}_{\circ\circ} = {}& -\frac{\hbar c}{2\pi}\int_0^\infty d\kappa \sum_{p=1}^\infty \frac{1}{p}\mathrm{Tr}[\sum_{n=0}^\infty (-1)^n(\mathbb{T}\mathbb{U}^I)^n\mathbb{T}(\mathbb{U}^{21}+\mathbb{U}^{I,21}) \\ & \times\sum_{n'=0}^\infty (-1)^{n'}(\mathbb{T}\mathbb{U}^I)^{n'}\mathbb{T}(\mathbb{U}^{12}+\mathbb{U}^{I,12})]^p.\end{aligned} \tag{4}$$

The trace acts on an alternating product of $\mathbb{T}$ and $\mathbb{U}$ matrices which describe scattering and free propagation of EM fluctuations, respectively. Multiple scatterings between an object and its image ($\mathbb{T}\mathbb{U}^I$) are followed by a propagation to the other object-image pair, either to the object ($\mathbb{U}^{21}$) or its image ($\mathbb{U}^{I,21}$), between which again multiple scatterings occur before the fluctuations are scattered back to the initial object or its image ($\mathbb{U}^{12}$ or $\mathbb{U}^{I,12}$) and the process repeats. This expansion is useful for small objects or large separations.

First, we consider the case of two identical, general polarizable objects near a wall in the dipole approximation, see Fig. 1. This case applies to ground state atoms and also to general objects at *large* separations. The separation between the objects is L, and the separation of each of them from the wall is H. In dipole approximation, the retarded limit of the interaction is described by the static electric (α_z, $\alpha_\parallel$) and magnetic (β_z, $\beta_\parallel$) dipole polarizabilities of the objects which can be different in the directions perpendicular (z) and parallel ($\parallel$) to the wall. The $\mathbb{T}$ matrix of the objects is diagonal and has finite elements only for the dipole channel (partial waves with $l=1$), given by $T^E_{10}=\frac{2}{3}\alpha_z\kappa^3$, $T^E_{1\,m}=\frac{2}{3}\alpha_\parallel\kappa^3$ for electric and $T^M_{10}=\frac{2}{3}\beta_z\kappa^3$, $T^M_{1\,m}=\frac{2}{3}\beta_\parallel\kappa^3$ for magnetic polarization with $m=\pm 1$. For atoms, the polarizability is much smaller than L^3, and hence it is sufficient to compute the interaction to second order in the polarizabilities. This amounts to neglecting all terms other than $p=1$ and $n=n'=0$ in Eq. (4). The resulting energy $\mathcal{E}_{\circ\circ}$ is then compared to the well-known Casimir-Polder (CP) interaction energy between two atoms (without the wall),

$$\mathcal{E}_{2,|}(L) = -\frac{\hbar c}{8\pi L^7}[33\alpha_\parallel^2 + 13\alpha_z^2 - 14\alpha_\parallel\beta_z + (\alpha\leftrightarrow\beta)], \tag{5}$$

which corresponds to the sequence $\mathbb{T}\mathbb{U}^{21}\mathbb{T}\mathbb{U}^{12}$ in Eq. (4). The total interaction energy is

$$\mathcal{E}_{\circ\circ}(L,H) = \mathcal{E}_{2,|}(L) + \mathcal{E}_{2,\backslash}(D,L) + \mathcal{E}_3(D,L), \tag{6}$$

with $D=\sqrt{L^2+4H^2}$. The two-body energy $\mathcal{E}_{2,\backslash}(D,L)$ comes from the sequence $\mathbb{T}\mathbb{U}^{I,21}\mathbb{T}\mathbb{U}^{I,12}$ in Eq. (4) and hence is the usual CP interaction between one atom and the image of the other atom (see Fig. 1). The change in the relative orientation of the objects with $\ell=L/D$ leads to the modified CP potential

$$\begin{aligned}\mathcal{E}_{2,\backslash}(D,L) = {}& -\frac{\hbar c}{8\pi D^7}[26\alpha_\parallel^2 + 20\alpha_z^2 - 14\ell^2(4\alpha_\parallel^2 - 9\alpha_\parallel\alpha_z + 5\alpha_z^2) \\ & + 63\ell^4(\alpha_\parallel-\alpha_z)^2 - 14(\alpha_\parallel\beta_\parallel(1-\ell^2) + \ell^2\alpha_\parallel\beta_z) \\ & + (\alpha\leftrightarrow\beta)].\end{aligned} \tag{7}$$

The three-body energy $\mathcal{E}_3(D,L)$ corresponds to the matrix products $\mathbb{T}\mathbb{U}^{21}\mathbb{T}\mathbb{U}^{I,12}$ and $\mathbb{T}\mathbb{U}^{I,21}\mathbb{T}\mathbb{U}^{12}$ in Eq. (4) and hence describes the collective interaction between the two objects and one image object. It is given by

$$\begin{aligned}\mathcal{E}_3(D,L) = {}& \frac{4\hbar c}{\pi}\frac{1}{L^3D^4(\ell+1)^5}[(3\ell^6+15\ell^5+28\ell^4+20\ell^3 \\ & + 6\ell^2-5\ell-1)(\alpha_\parallel^2-\beta_\parallel^2) \\ & - (3\ell^6+15\ell^5+24\ell^4-10\ell^2-5\ell-1)(\alpha_z^2-\beta_z^2) \\ & + 4(\ell^4+5\ell^3+\ell^2)(\alpha_z\beta_\parallel-\alpha_\parallel\beta_z)].\end{aligned} \tag{8}$$

For isotropic electric polarizable atoms this result agrees

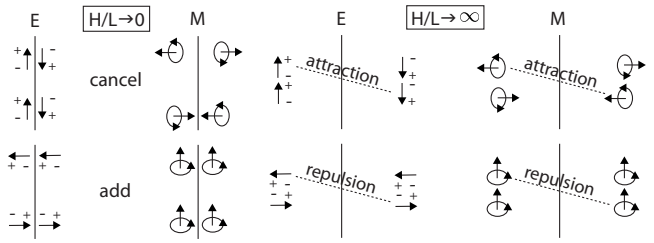

FIG. 2. Typical orientations of electric (e) and magnetic (m) dipoles and image dipoles for $H/L \to 0$ and $H/L \to \infty$.

with that of Ref. [2]. It is instructive to consider the two limits $H \ll L$ and $H \gg L$. For $H \ll L$ one has $D \to L$ and the two-body potentials are identical, $\mathcal{E}_{2,\backslash}(L,L) = \mathcal{E}_{2,|}(L)$. The three-body energy becomes

$$\mathcal{E}_3(L,L) = -\frac{\hbar c}{4\pi L^7}[-33\alpha_\parallel^2 + 13\alpha_z^2 + 14\alpha_\parallel\beta_z - (\alpha \leftrightarrow \beta)]. \tag{9}$$

The total energy $\mathcal{E}_\infty$ is now twice the energy of Eq. (5) plus the energy of Eq. (9) and hence $\mathcal{E}_\infty$ becomes the CP potential of Eq. (5) with the replacements $\alpha_z \to 2\alpha_z$, $\alpha_\parallel \to 0$, $\beta_z \to 0$, $\beta_\parallel \to 2\beta_\parallel$. The two-body and three-body contributions add constructively or destructively, depending on the relative orientation of a dipole and its image which together form a dipole of zero or twice the original strength (see Fig. 2). For $H \gg L$ the leading correction to the CP potential of Eq. (5) comes from the three-body energy which in this limit becomes (up to order H^{-6})

$$\mathcal{E}_3(H,L) = \frac{\hbar c}{\pi}\left[\frac{\alpha_z^2 - \alpha_\parallel^2}{4L^3H^4} + \frac{9\alpha_\parallel^2 - \alpha_z^2 - 2\alpha_\parallel\beta_z}{8LH^6} - (\alpha \leftrightarrow \beta)\right]. \tag{10}$$

The signs of the polarizabilities in the leading term $\sim H^{-4}$ can be understood from the relative orientation of the dipole of one atom and the image dipole of the other atom, see Fig. 2. If these two electric (magnetic) dipoles are almost perpendicular to their distance vector they contribute attractively (repulsively) to the potential between the two original objects. If these electric (magnetic) dipoles are almost parallel to their distance vector they yield a repulsive (attractive) contribution. For isotropic polarizabilities the leading term of Eq. (10) vanishes and the electric (magnetic) part $\sim H^{-6}$ of the three-body energy is always repulsive (attractive).

The above results show how the force between the two particles varies with H. If the two particles have only either α_z or $\beta_\parallel$ polarizability, their attractive force is *reduced* when they approach the wall from large H due to the repulsive three-body interaction. At close proximity to the wall the fluctuations of the dipole and its image add up to yield a force between the particles that is *enhanced* by a factor of 4 compared to the force for $H \to \infty$. Corresponding arguments show that the force between particles with either $\alpha_\parallel$ or β_z polarizability is enhanced at large H and reduced to zero for $H \to 0$. This proves that the force between particles which both have either of the four polarizabilities is always nonmonotonic. The situation can be different if more than one polarizability is finite, especially for isotropic particles. In the latter case all contributions (electric, magnetic, mixed) are enhanced for $H \to 0$ and only the electric term is reduced at large H so that only the electric part gives a nonmonotonic force. In general, the monotonicity property depends on the relative strength and anisotropy of the electric and magnetic polarizabilities.

Second, we study two macroscopic perfect metallic spheres of radius R for the same geometry as before where the lengths L and H are measured now from the centers of the spheres, see Fig. 1. Here we do not limit the analysis to large separations but consider arbitrary distances and include higher-order multipole moments than just dipole polarizability. The $\mathbb{T}$ matrix is diagonal and the elements $T^M_{lm} = (-1)^l \frac{\pi}{2} I_{l+1/2}(\kappa R)/K_{l+1/2}(\kappa R)$, $T^E_{lm} = (-1)^l \frac{\pi}{2}[I_{l+1/2}(\kappa R) + 2\kappa R I'_{l+1/2}(\kappa R)]/[K_{l+1/2}(\kappa R) + 2\kappa R K'_{l+1/2}(\kappa R)]$ are given in terms of the modified Bessel functions I_ν, K_ν. First, we expand the energy in powers of R by using Eq. (4) which implies that we expand the $\mathbb{T}$ matrices for small frequencies but use the exact expressions for the $\mathbb{U}$ matrices. For $R \ll L$, H, and arbitrary H/L the result for the force can be written as

$$F = \frac{\hbar c}{\pi R^2}\sum_{j=6}^{\infty} f_j(H/L)\left(\frac{R}{L}\right)^{j+2}. \tag{11}$$

The functions f_j can be computed exactly. We have obtained them up to $j=11$ and the first three are (with $s \equiv \sqrt{1+4h^2}$)

$$f_6(h) = -\frac{1}{16h^8}[s^{-9}(18 + 312h^2 + 2052h^4 + 6048h^6 + 5719h^8) + 18 - 12h^2 + 1001h^8], \quad f_7(h) = 0, \tag{12}$$

$$f_8(h) = -\frac{1}{160h^{12}}[s^{-11}(6210 + 140554h^2 + 1315364h^4 + 6500242h^6 + 17830560h^8 + 25611168h^{10} + 15000675h^{12}) - 6210 - 3934h^2 + 764h^4 - 78h^6 + 71523h^{12}]. \tag{13}$$

The coefficient f_7 of R^7 vanishes since a multipole of order l contributes to the $\mathbb{T}$ matrix at order R^{2l+1} so that beyond the two-dipole term $\sim R^6$ the next term comes from a dipole ($l=1$) and a quadrupole ($l=2$), yielding f_8. For $H \gg L$ one has $f_6(h) = -1001/16 + 3/(4h^6) + O(h^{-8})$, $f_8(h) = -71523/160 + 39/(80h^6) + O(h^{-8})$ so that the wall induces weak repulsive corrections. For $H \ll L$, $f_6(h) = -791/8 + 6741h^2/8 + O(h^4)$, $f_8(h) = -60939/80 + 582879h^2/80 + O(h^4)$ so that the force amplitude decreases when the spheres are moved a small distance away from the wall. This proves the existence of a minimum in the force amplitude as a function of H/R for fixed, sufficiently small R/L. We note that all $f_j(h)$ are finite for $h \to \infty$ but some diverge for $h \to 0$, e.g., $f_9 \sim f_{11} \sim h^{-3}$, making them important for small H.

To obtain the interaction at smaller separations or larger radius, we have computed the energy $\mathcal{E}_\infty$ and force $F = -\partial\mathcal{E}_\infty/\partial L$ between the spheres numerically. For the energy, we have computed the last determinant of Eq. (3) and the

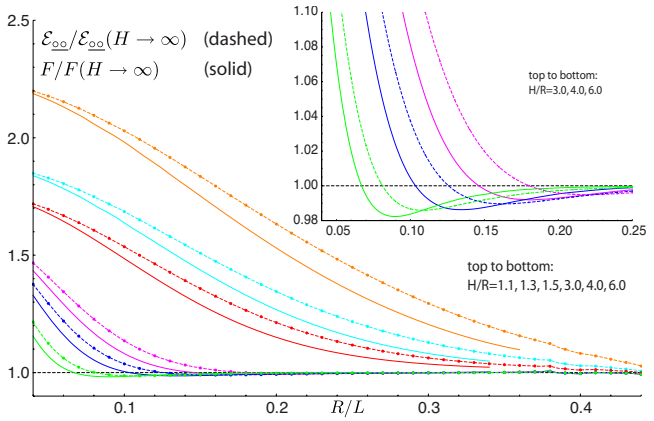

FIG. 3. (Color online) Numerical results for the potential energy (dashed curves) and force (solid curves) between two spheres as function of R/L for different sidewall separations H/R. Both force and energy are normalized to their values in the absence of the sidewall. Inset: magnification of behavior for small R/L.

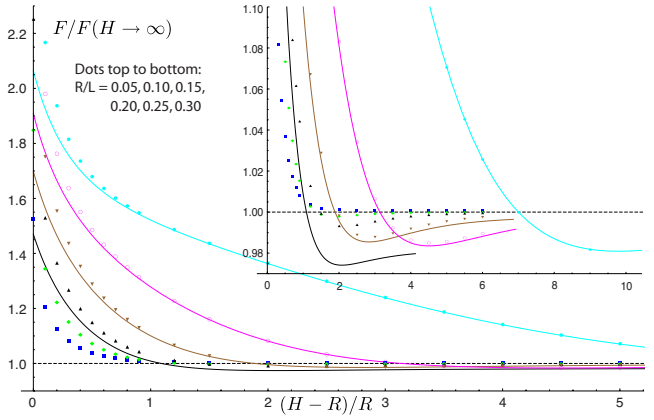

FIG. 4. (Color online) Numerical results for the force (dots) between two spheres as function of the sidewall separation H/R for different sphere separations R/L. Shown are also the analytical results of Eq. (11), including terms up to $j=10$ for $R/L\leq 0.2$ (solid curves). Inset: magnification of the nonmonotonicity.

integral over κ of Eq. (1) numerically. The force is obtained by polynomial interpolation of the data for the energy. The matrices are truncated at a sufficiently large number of partial waves (with a maximum truncation order $l_{max}=17$ for the smallest separation) so that the relative accuracy of the values for $\mathcal{E}_{\circ\circ}$ is $\approx 10^{-3}$. The data for $H/R=1$ are obtained by extrapolation in l_{max}. The results are shown in Figs. 3 and 4. In order to show the effect of the wall, the figures display the energy and force normalized to the results for two spheres without a wall. Figure 3 shows the energy and force as a function of the (inverse) separation between the spheres for different fixed wall distances. The proximity of the wall generally increases the interaction energy and the force between the two spheres. The effect is more pronounced, the further the two spheres are separated. For sufficiently large H/R, the energy and force ratios are nonmonotonic in L and can be slightly smaller than they would be in the absence of the wall. Figure 4 shows the force between the two spheres as a function of the wall distance for fixed L. When the spheres approach the wall, the force first decreases slightly if $R/L \lesssim 0.3$ and then increases strongly under a further reduction in H. For $R/L \gtrsim 0.3$ the force increases monotonically as the spheres approach the wall. This agrees with the prediction of the large distance expansion. The expansion of Eq. (11) with $j=10$ terms is also shown in Fig. 4 for $R/L\leq 0.2$. Its validity is limited to large L/R and not too small H/R; it fails completely for $R/L>0.2$ and hence is not shown in this range.

Since experimentalists have made great progress in measuring the Casimir force between two objects in past years [13–29], it can be expected that measuring three-body forces may as well be feasible in the future. Our results for macroscopic spheres indicate an interesting modification of the force between two spheres due to the presence of a sidewall. Also, the force between two spheres is enhanced by the proximity of the sidewall; thus a sidewall may make the observation of Casimir forces between small particles easier. Of course, for realistic predictions, material and temperature dependence, surface roughness, etc. have to be taken into account, but these considerations lay outside the scope of our investigation. The dependence on the anisotropy of polarizabilities applies not only to atoms but to general polarizable objects and suggests interesting effects for objects of nonspherical shape, e.g., spheroids. Our results for isotropic atoms are also potentially relevant to the interaction between trapped Bose-Einstein condensates and a surface [20] at close surface separations. The results for macroscopic spheres could be important for the design of nanomechanical devices where small components operate in close vicinity to metallic boundaries.

We acknowledge helpful discussions with N. Graham, R. L. Jaffe, and M. Kardar, and the hospitality of the Institute of Theoretical Physics, University of Cologne. This work was supported by projects MOSAICO, UCM/PR34/07-15859, and a PFU MEC grant (P.R.), National Science Foundation (NSF) Grant No. DMR-08–03315 (S.J.R.), and by DFG through Grant No. EM70/3 (T.E.).

[1] V. A. Parsegian, *Van der Waals Forces* (Cambridge University Press, Cambridge, England, 2005).
[2] E. A. Power and T. Thirunamachandran, Phys. Rev. A **25**, 2473 (1982).
[3] G. Feinberg, Phys. Rev. B **9**, 2490 (1974).
[4] T. Emig, N. Graham, R. L. Jaffe, and M. Kardar, Phys. Rev. Lett. **99**, 170403 (2007).
[5] A. W. Rodriguez, M. Ibanescu, D. Iannuzzi, F. Capasso, J. D. Joannopoulos, and S. G. Johnson, Phys. Rev. Lett. **99**, 080401 (2007).

[6] S. J. Rahi, A. W. Rodriguez, T. Emig, R. L. Jaffe, S. G. Johnson, and M. Kardar, Phys. Rev. A **77**, 030101(R) (2008).
[7] S. J. Rahi, T. Emig, R. L. Jaffe, and M. Kardar, Phys. Rev. A **78**, 012104 (2008).
[8] T. Emig, J. Stat. Mech.: Theory Exp. (2008) P04007.
[9] M. J. Renne, Physica **56**, 125 (1971).
[10] R. Balian and B. Duplantier, Ann. Phys. (N.Y.) **112**, 165 (1978).
[11] A. Bulgac and A. Wirzba, Phys. Rev. Lett. **87**, 120404 (2001).
[12] O. Kenneth and I. Klich, Phys. Rev. B **78**, 014103 (2008).
[13] S. K. Lamoreaux, Phys. Rev. Lett. **78**, 5 (1997).
[14] U. Mohideen and A. Roy, Phys. Rev. Lett. **81**, 4549 (1998).
[15] A. Roy, C.-Y. Lin, and U. Mohideen, Phys. Rev. D **60**, 111101(R) (1999).
[16] T. Ederth, Phys. Rev. A **62**, 062104 (2000).
[17] H. B. Chan, V. A. Aksyuk, R. N. Kleiman, D. J. Bishop, and F. Capasso, Science **291**, 1941 (2001).
[18] F. Chen, U. Mohideen, G. L. Klimchitskaya, and V. M. Mostepanenko, Phys. Rev. Lett. **88**, 101801 (2002).
[19] V. Druzhinina and M. DeKieviet, Phys. Rev. Lett. **91**, 193202 (2003).
[20] D. M. Harber, J. M. Obrecht, J. M. McGuirk, and E. A. Cornell, Phys. Rev. A **72**, 033610 (2005).
[21] F. Chen, G. L. Klimchitskaya, V. M. Mostepanenko, and U. Mohideen, Phys. Rev. Lett. **97**, 170402 (2006).
[22] D. E. Krause, R. S. Decca, D. López, and E. Fischbach, Phys. Rev. Lett. **98**, 050403 (2007).
[23] R. S. Decca, D. López, E. Fischbach, G. L. Klimchitskaya, D. E. Krause, and V. M. Mostepanenko, Phys. Rev. D **75**, 077101 (2007).
[24] F. Chen, G. L. Klimchitskaya, V. M. Mostepanenko, and U. Mohideen, Phys. Rev. B **76**, 035338 (2007).
[25] J. N. Munday and F. Capasso, Phys. Rev. A **75**, 060102(R) (2007).
[26] H. B. Chan, Y. Bao, J. Zou, R. A. Cirelli, F. Klemens, W. M. Mansfield, and C. S. Pai, Phys. Rev. Lett. **101**, 030401 (2008).
[27] W. J. Kim, M. Brown-Hayes, D. A. R. Dalvit, J. H. Brownell, and R. Onofrio, Phys. Rev. A **78**, 020101(R) (2008).
[28] G. Palasantzas, P. J. van Zwol, and J. Th. M. De Hosson, Appl. Phys. Lett. **93**, 121912 (2008).
[29] J. N. Munday, F. Capasso, and V. A. Parsegian, Nature (London) **457**, 170 (2009).